Improved Measurement of Particulate Retention in Simulated Stress Corrosion Cracks

Spent Fuel and Waste Disposition

Prepared for
US Department of Energy
Spent Fuel and Waste Science and Technology

S.G. Durbin
E.R. Lindgren
R.J.M. Pulido
K.R. Ford

Sandia National Laboratories
March 15, 2019
Milestone No. M4SF-19SN010201046
SAND2019-2917 R

Prepared by
Sandia National Laboratories
Albuquerque, New Mexico 87185 and Livermore, California 94550

Sandia National Laboratories is a multimission laboratory managed and operated by National Technology and Engineering Solutions of Sandia, LLC, a wholly owned subsidiary of Honeywell International, Inc., for the U.S. Department of Energy's National Nuclear Security Administration under contract DE-NA0003525.

ABSTRACT

This report documents proposed improvements to an apparatus for measuring flow rates and aerosol retention in stress corrosion cracks (SCCs). The potential for SCCs in canister walls is a concern for dry cask storage systems for spent nuclear fuel. Some of the canisters in these systems are backfilled to significant pressures to promote heat rejection via internal convection. Pressure differentials covering the upper limit of commercially available dry cask storage systems are the focus of the current test assembly. Initial studies will be conducted using engineered microchannels with characteristic dimensions expected in SCCs that hypothetically could form in dry storage canister walls.

In a previous study, an apparatus and procedures were developed and implemented to investigate aerosol retention in a simple microchannel with an SCC-like opening of 28.9 μm (0.00110 in.). The width was 12.7 mm (0.500 in.), and the length was 8.86 mm (0.349 in.). These initial results indicated 44% of the aerosols available for transmission were retained upstream of microchannel. However, limitations in the aerosol instruments available at the time of the preliminary study introduced known biases into the measurements. While these biases were identified and quantified, their presence introduced unwanted degrees of freedom into the measurements and reduced accuracy. Because these aerosol particle sizers (APS) were limited to sampling at atmospheric pressure, a mass flow controller was used to supply the sample upstream of the crack to the APS. The average line loss across all particle sizes for this mass flow controller was 50%. The sample downstream of the crack was delivered via a mass flow meter and caused a line loss of 20%. Another source of bias was using separate (but identical) instruments to measure the aerosols upstream and downstream of the microchannel, which could register up to 40% different when measuring the same sample stream.

The experience of conducting the preliminary study highlighted the need for improvements in the experimental approach that would eliminate these biases and benefit future studies. An aerosol analyzer has been identified and ordered that is ideally suited for this study and should substantially mitigate these biases. Moving forward in the near term, the same simple microchannel will be further investigated using the improved aerosol instrumentation. Additionally, an offset microchannel with a step in the flow path will be designed and fabricated for similar testing. Looking out further, the capability to produce and test laboratory generated SCCs will be developed.

This page is intentionally left blank.

ACKNOWLEDGEMENTS

The authors would like to gratefully acknowledge the hard work and commitment to excellence of Andres Sanchez, Shannon Zubersky, William Chavez, and Greg Koenig, which made the success of this project possible.

This work was conducted under the Department of Energy Spent Fuel and Waste Disposition campaign. Sylvia Saltzstein (8845) and Geoff Freeze (8843) are to be commended for exceptional project leadership.

This page is intentionally left blank.

CONTENTS

This page is intentionally left blank.

LIST OF FIGURES

LIST OF TABLES

ACRONYMS

AED	aerodynamic equivalent diameter
APS	aerosol particle sizer
DCSS	dry cask storage systems
DOE	US Department of Energy
EDM	electrical discharge machining
FY	fiscal year
PWR	pressurized water reactor
SCC	stress corrosion crack
SFWD	Spent Fuel and Waste Disposition
slpm	standard liter per minute
SNF	spent nuclear fuel

This page is intentionally left blank.

IMPROVED MEASUREMENT OF PARTICULATE RETENTION IN SIMULATED STRESS CORROSION CRACKS

This report fulfills milestone M4SF-19SN010201046 in the Stress Corrosion Cracking and Dry Storage Investigations work package (SF-19SN01020104). This work was sponsored under the Department of Energy's (DOE) Office of Nuclear Energy Spent Fuel and Waste Disposition (SFWD) campaign.

1 INTRODUCTION

Dry cask storage systems (DCSS) for spent nuclear fuel (SNF) are designed to provide a confinement barrier that prevents the release of radioactive material, maintain SNF in an inert environment, provide radiation shielding, and maintain subcriticality conditions. SNF is initially stored in pools of water for cooling where the water also provides radiation shielding. As these pools get closer to capacity, DCSSs are becoming the primary alternative for interim storage. After sufficient cooling in pools, SNF is loaded into a canister, which is then welded shut and placed inside a storage cask. The DCSS is then decontaminated and dried, and ultimately transferred to a storage location. Figure 1 shows the major components of a DCSS for spent nuclear fuel.

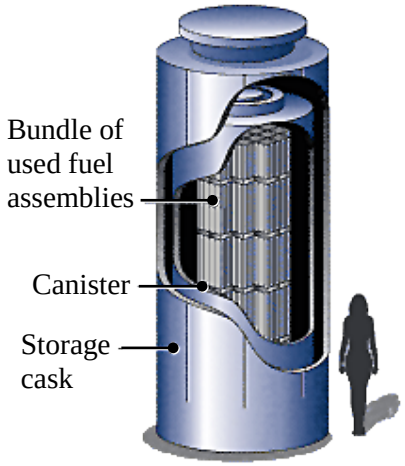

Source: https://www.nrc.gov/waste/spent-fuel-storage/diagram-typical-dry-cask-system.html

Figure 1. Typical dry cask storage system.

Typically, the canisters are made of stainless steel. The open volume between the canister and the cask allows passive ventilation from outside air, which can impart dust that collects on the surfaces of the canister. As the SNF cools, salts contained in the dust may deliquesce to form concentrated brines, which may contain corrosive species such as chlorides. These species are capable of causing localized corrosion, called pitting. With sufficient stresses, these pits can evolve into stress corrosion cracks (SCCs), which could penetrate through the canister wall and allow communication from the interior of the canister to the external environment [Schindelholz, 2017]. If the internal pressure of the canister is greater than ambient pressure at the time the SCC fully penetrates the canister wall, the internal backfill gas will blowdown into the environment. This initial blowdown is the subject of the proposed studies outlined in this report.

1.1 Objective

The purpose of this on-going research is to explore the flow rates through and the aerosol retention in SCCs. Initial testing will employ engineered slots with characteristic dimensions similar to those in SCCs

as analogs. A new, advanced approach is being explored for future testing of actual SCCs grown under accelerated, laboratory conditions.

Improvements are being made to the experimental setup to increase measurement sensitivity and accuracy. A new aerosol analysis system is being integrated into the experimental system that can directly monitor native pressure upstream samples, which will eliminate a large source of aerosol loss previously found when the sample pressure was reduced before analysis [Durbin *et al.*, 2018]. Furthermore, this high-pressure aerosol characterization system, Palas Promo® 3000 HP, is designed to opto-mechanically switch between monitoring upstream and downstream sensing elements offering nearly simultaneous measurements and eliminate the instrument bias seen in previous testing [Durbin *et al.*, 2018].

1.2 Previous Studies

The data obtainable from the measurement of particulate segregation in flows through open channels has significance in multiple fields. Studies include particle penetration through building cracks [Lewis, 1995; Liu and Nazaroff, 2003; Mosley *et al.*, 2001] to nuclear reactor safety [Powers, 2009], and more recently, storage and transportation of spent nuclear fuel in dry casks. Study of these systems contribute to the understanding of particulate segregation through small channels as functions of particle size, channel dimensions, and differential pressures.

Previous work has contributed to the characterization of particulate segregation across channel flow for a range of particle sizes in aerosols. Lewis [Lewis, 1995] was motivated by a lack of empirical studies to support the development of protection factors against solid particles for enclosures. This protection factor was taken as the ratio of the dose of an outside concentration of particulates to the dose accumulated inside an enclosure for a specified time, with the doses defined as concentration-time integrals. Models were derived describing the total transport fraction of particles across a rectangular slot into an enclosure as functions of particle size, differential pressures, and slot heights. Lewis described an experimental apparatus with synthesized aerosols (containing either talc, aluminum oxide, titanium oxide, various silica powders, or ambient dust) mixed in a chamber containing an enclosure with a rectangular slot open to the chamber. A differential pressure was established between the chamber and the enclosure. Protection factors were found by comparing mass concentration values inside and outside the enclosure over a given time. The primary observations here were the decrease in total transport fraction with increasing particle size from 1-10 µm as well as a decrease in protection factor (corresponding to an increase in total transport fraction) with increasing differential pressures and slot heights.

Liu and Nazaroff [Liu and Nazaroff, 2003] conducted experiments of aerosol flow through rectangular slots using various building materials, including aluminum, brick, concrete, and wood. The slot heights were 0.25 mm and 1 mm, which are large compared to the micron- to submicron-sized particles they flowed through the cracks. They obtained data for particle penetration (defined as the ratio of downstream to upstream particle concentration), related to total transport fraction, as a function of particle size and found that, for 0.25 mm cracks, particle sizes between 0.1-1 µm achieved penetration factors near unity, while smaller and larger particles showed diminished penetration factors for pressure differentials of 4 and 10 Pa. Meanwhile, for 1 mm slot heights, the penetration factors were near unity for the majority of the particle size distribution. Their results matched closely with models they created from analysis of particle penetration through simplified cracks [Liu and Nazaroff, 2001] and had similar qualitative conclusions to Lewis's work.

Mosley *et al.* [Mosley *et al.*, 2001] studied particle penetration through a 0.508 mm slot height between aluminum plates with particles of aerodynamic equivalent diameters (AED) from 0.1 to 5 µm. They found penetration factors close to unity for particle sizes between 0.1-1 µm, with a sharp drop-off in penetration factor for particle sizes larger than 1 µm for pressure differentials between 2 and 20 Pa – this was consistent with Liu and Nazaroff's results when considering the order of magnitude of the pressure differentials and particle size distributions.

1.3 Current Study and Recent Findings

The motivation behind the previous work by others was based on ambient particle penetration of enclosures and the amount of particles subject to environmental release, with slot heights and pressure differentials corresponding to conditions typically associated with building cracks and pressure differences between indoor and outdoor environments, respectively. However, the channel dimensions considered did not apply to the channel geometry associated with cracks from potential corrosion of dry storage casks. The literature reports typical SCC heights to be around 16 to 30 μm [EPRI, 2017, EPRI, 2014, Meyer, 2013] and internal pressures of 100 to 760 kPa (14.5 to 110 psig) [EPRI, 2017] for a range of cask models. Therefore, an apparatus and procedures were developed and implemented to investigate aerosol retention in a simple microchannel with a gap of 29 microns and initial pressure differential of 700 kPa. Preliminary results indicated 44% of the aerosols available for transmission were retained upstream of the microchannel [Durbin *et al.*, 2018].

The experience of conducting the preliminary study highlighted the need for improvements in the aerosol measurements. Biases in the preliminary aerosol measurements were found to be due to two sources. One source was known aerosol line losses that occurred in both sample trains. The high-pressure sample upstream of the crack was reduced to ambient pressure for analysis by a mass flow controller, which resulted in a 50% line loss. The low-pressure sample passed through a mass flow meter resulting in a 20% line loss. Another identified source of bias was using separate (but identical) aerosol particle sizers (APSs) to measure the aerosols upstream and downstream of the microchannel. These APSs registered up to a 40% difference when measuring the same sample [Durbin *et al.*, 2018].

An aerosol analyzer has been identified and ordered that is ideally suited for this study and should eliminate previously observed biases. The Palas Promo® 3000 HP is fiber optically coupled to two welas® 2070 high pressure aerosol sensors. The high-pressure aerosol sensor directly samples gas streams at native pressures up to 1000 kPa. Rapid fiber optic switching allows a single instrument to analyze the upstream and downstream aerosol sensors in quasi-simultaneous fashion. Thus, instrument bias is eliminated, and sample line losses are substantially minimized.

Moving forward in the near term, the same simple microchannel will be further investigated using the improved aerosol instrumentation. Additionally, an offset microchannel with a step in the flow path will be designed and fabricated (see Section 2.2.2) for similar testing. Laboratory-generated SCCs will be explored for future testing as well (see Section 2.2.3).

This page is intentionally left blank.

2 APPARATUS AND PROCEDURES

The experimental approach adopted for these studies is similar to previous studies [Lewis, 1995; Mosley *et al.*, 2001; and, Liu and Nazaroff, 2001 and 2003] in that aerosol analyzers are used to characterize the particle size distribution and concentration present in the gas before and after flowing through a simulated crack. Because these previous studies considered aerosol transport through building walls or containment structures, the focus was on flows through relatively wide and long slots driven by constant low pressure drops. In the present study, consideration is given to aerosol transport through dry storage canister walls. Here, the focus is on much narrower and shorter microchannels that represent SCCs through the canister wall driven by initially higher pressure drops. Furthermore, the pressure drop is not constant but transient to simulate the blowdown from canister depressurization.

2.1 General Construction

The general layout of the experimental setup is illustrated in Figure 2 and Figure 3. A 0.908 m^3 (240 gal) pressure tank is used to simulate the canister. The tank will be pressurized and loaded with a measured amount of aerosols. The valve from the tank to the test section will be opened, and the gas and aerosols will be allowed to naturally blowdown through the microchannel. Flow from the tank into the test section will be measured by a mass flow meter. The engineered microchannel, simulating a crack, will be mounted in the middle of the test section. A sample stream will be drawn from the high-pressure upstream and low-pressure downstream side of the test microchannels (either as engineered orifices or eventually fabricated SCC specimens) for aerosol size and concentration characterization using identical welas® 2070 high pressure aerosol sensors monitored by a single Palas Promo® 3000 HP analyzer. Mass flow meters measure the sample flow leaving each of the aerosol sensors. Pressure is monitored on the upstream and downstream sides of the microchannel using pressure transducers. A low pressure drop HEPA filter will be used to remove all aerosols from the exhaust stream if needed.

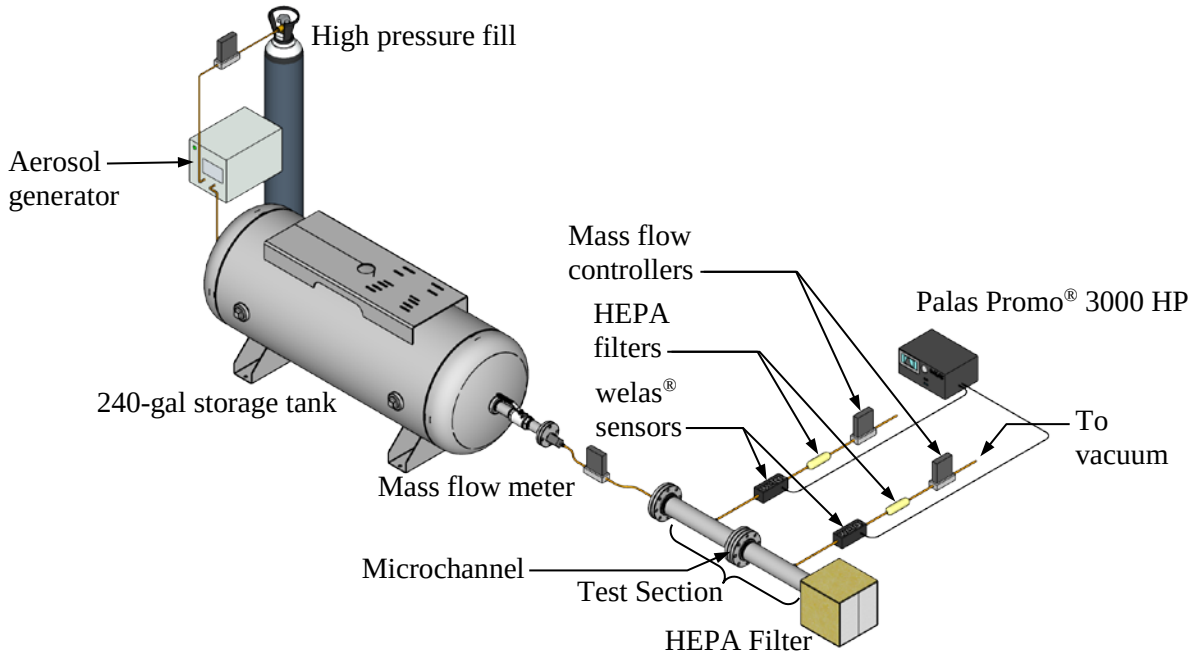

Figure 2. General layout of the experimental apparatus.

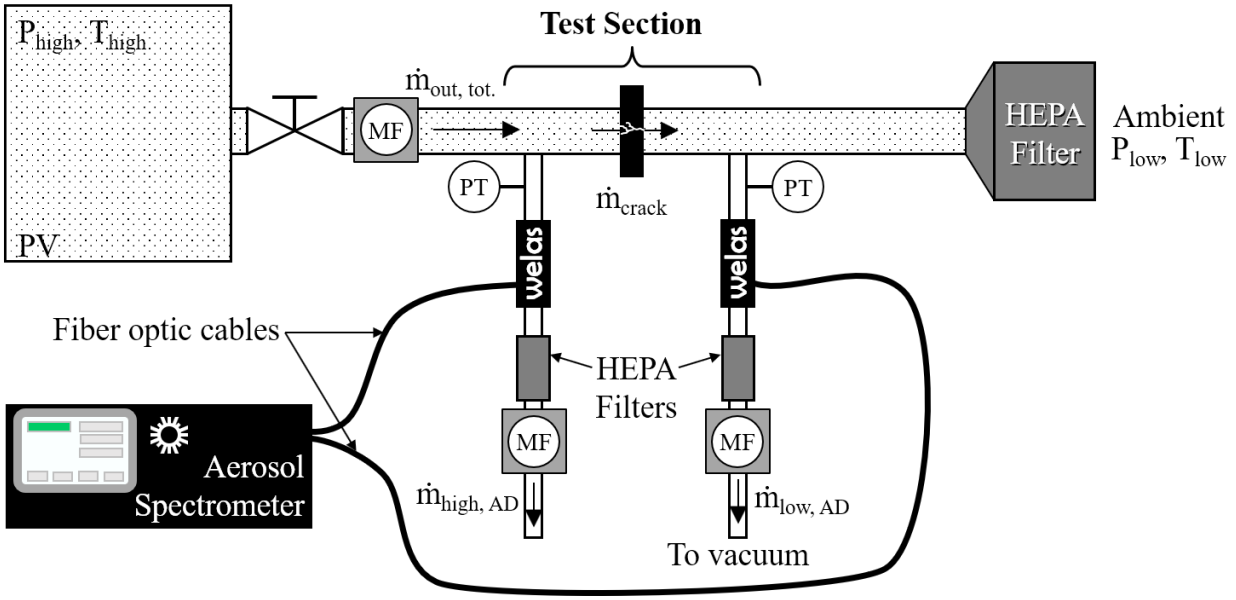

Figure 3. Schematic of the apparatus showing the major components.

2.2 Design of the Microchannel

2.2.1 Simple Slot Orifice

An engineered microchannel has been fabricated from paired high-precision Mitutoyo gage blocks. The microchannel was machined into the surface of one gage block using electrical discharge machining (EDM). The mounting holes were also cut using wire EDM. As shown in Figure 4 the dimensions of the microchannel are 12.7 mm (0.500 in.) wide, 8.86 mm (0.349 in.) long and an average of 28.9 μm (0.0011 in.) deep. The paired halves of the gage blocks are bolted together to form the microchannel held in a mounting assembly as detailed in Figure 5. An isometric view of the microchannel mounted to the flow flange is shown in Figure 6.

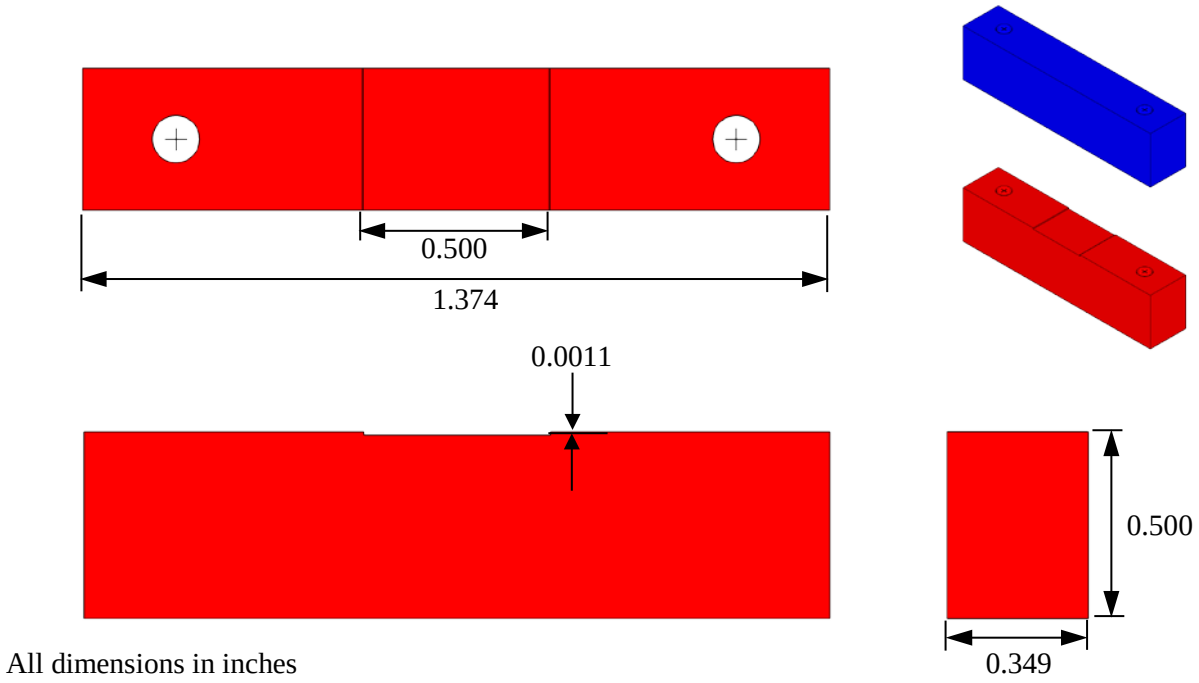

Figure 4. Schematic of the microchannel assembly.

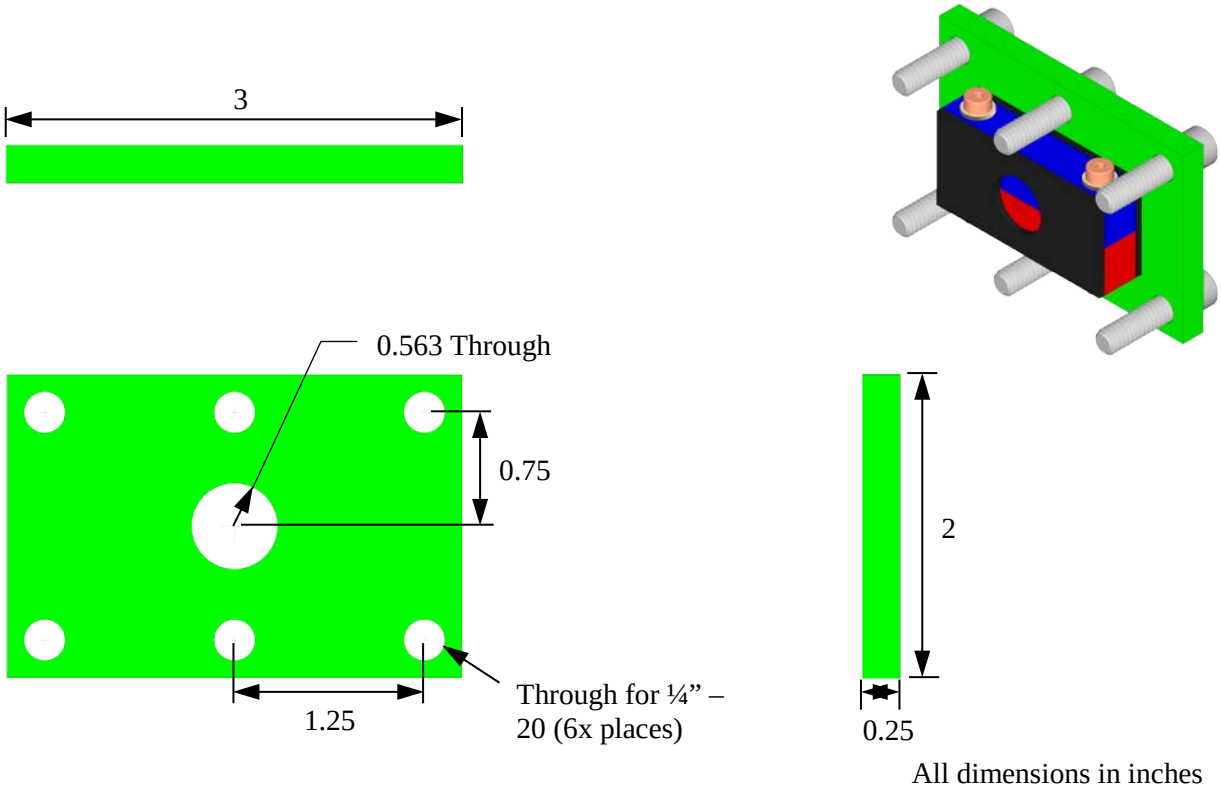

Figure 5. Details of the microchannel mounting assembly.

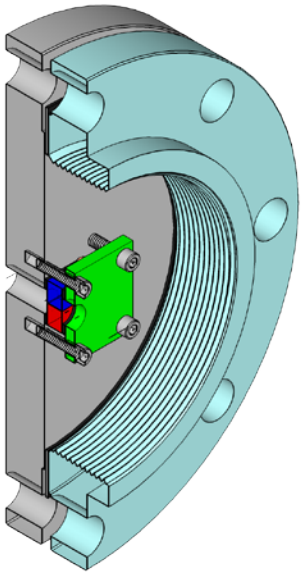

Figure 6. Isometric cutaway showing the microchannel mounted to the flow flange.

Figure 7 shows profilometry of the microchannel on both sides of the as-built microchannel. These scans represent approximately 1.2 mm (0.047 in.) of the overall 12.7 mm (0.500 in.) slot, or 9%. The average step height based on these measurements is 28.9 µm (0.0011 in.). These profiles were taken with a Keyence VK-X100 laser scanning microscope.

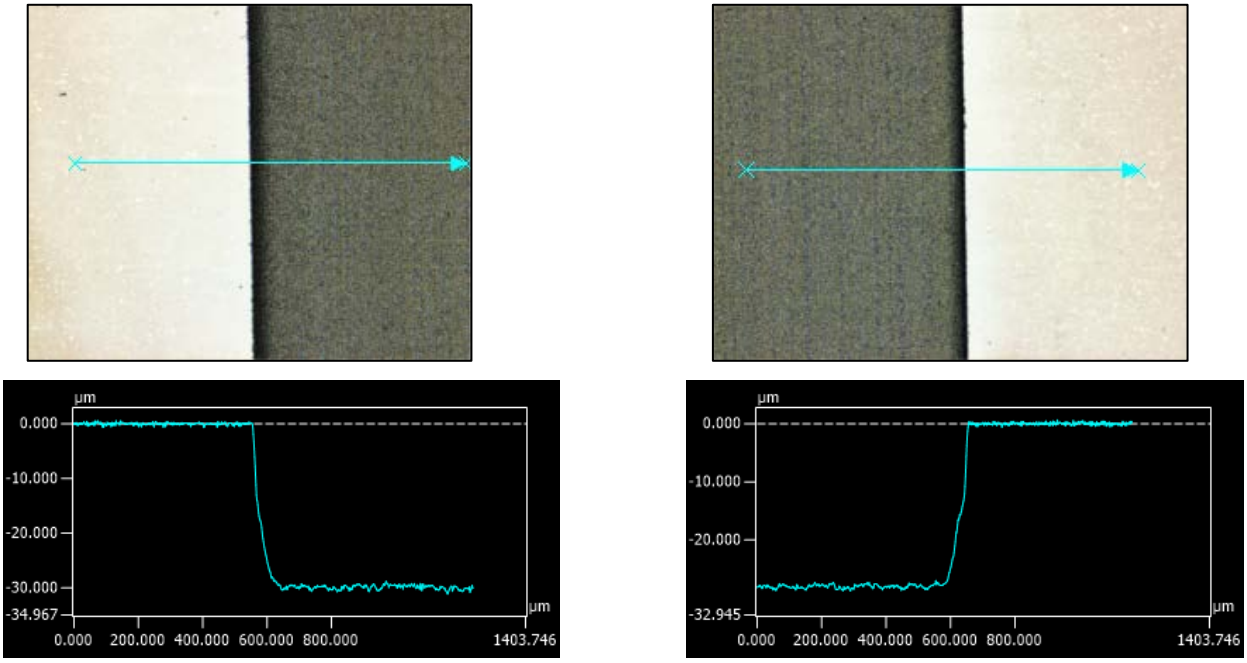

Area average step height 29.9 µm

Area average step height 27.9 µm

Figure 7. Profilometry of the microchannel orifice.

During the profilometry the surface roughness of the microchannel was also characterized with the Keyence VK-X100 laser scanning microscope. The results of the surface roughness characterization are given in Figure 8. In the embedded tables, S_a is the arithmetical mean height of the shown areas and is defined as the average of the difference between each surface point measurement and the mean plane of the surface. The root-mean-square height, S_q, is equivalent to the standard deviation of heights. Area2 is the microchannel surface and Area1 is the adjoining gage surface. By all measures the surface roughness of the microchannel was roughly twice that of the gage block surface.

Left Side 10×

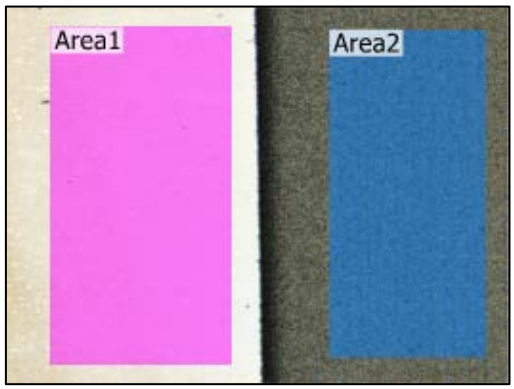

	S_a (µm)	S_q (µm)
Area1	0.213	0.275
Area2	0.408	0.520

Right Side 10×

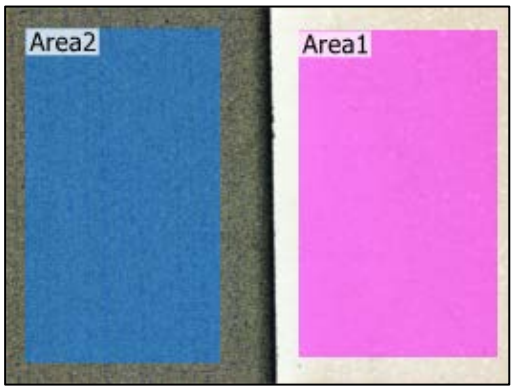

	S_a (µm)	S_q (µm)
Area1	0.238	0.300
Area2	0.386	0.494

Figure 8. Surface roughness characterizations.

2.2.2 Offset Slot Orifice

An additional complexity being considered for testing is a slot orifice with a single offset step. This geometry will allow the introduction of a simple and known tortuosity in the flow path. The offset slot orifice configuration is shown in Figure 9.

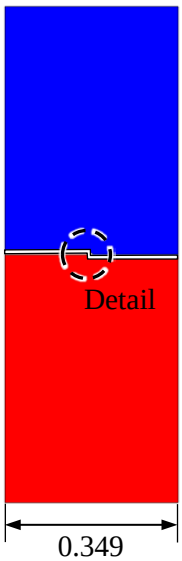

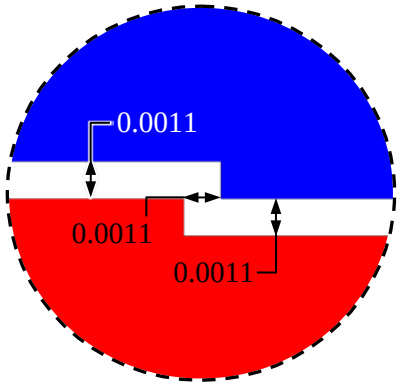

Detail

All dimensions in inches

Figure 9. Cross section of slot orifice with a simple offset.

2.2.3 Future Testing of SCC Geometries

The growth of realistic SCCs has been successfully accelerated under laboratory conditions [EPRI, 2018]. The method requires creating a tensile stress field through-wall in a specimen and exposing it to an acidified potassium tetrathionate ($K_2S_4O_6$) solution. The SCC is induced by the sulphur oxyanion species in the solution over a relatively short period [Breimesser, *et al.*, 2012].

Careful placement of an engineered welding pattern may be able produce the required prototypic through-wall tensile stress for growing SCCs as illustrated in Figure 10. To produce the desired stress field, a region near the center of a sample plate is subjected to a specific weld schedule. The sample is then masked and a small region in the heat-affected zone is exposed to the potassium tetrathionate solution. The resulting sample plate with a through-wall crack is designed to be mounted in a test fixture as shown in Figure 11. Testing would be conducted by the same procedures used for the engineered microchannels.

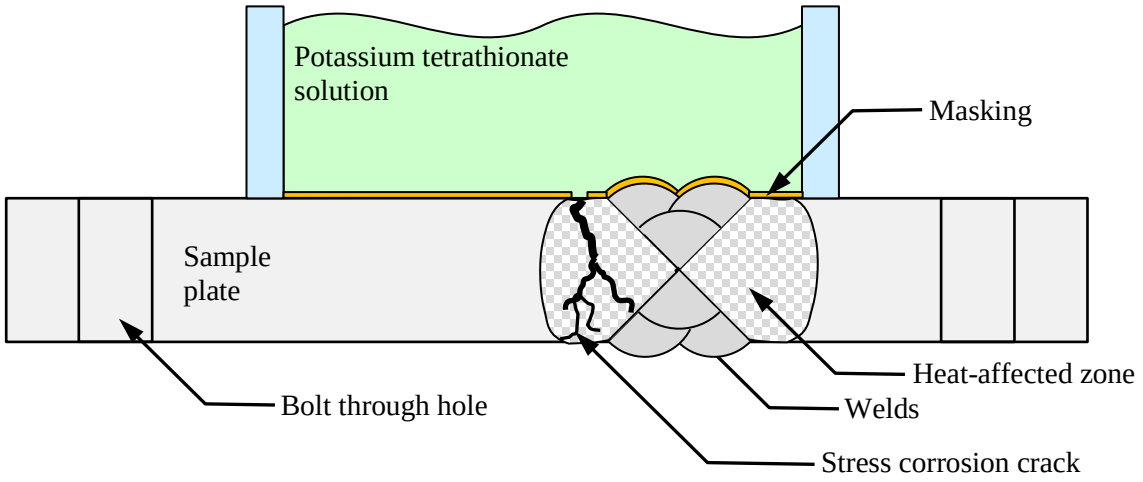

Figure 10. Cross section of a sample plate for flow testing configured to grow an accelerated stress corrosion crack.

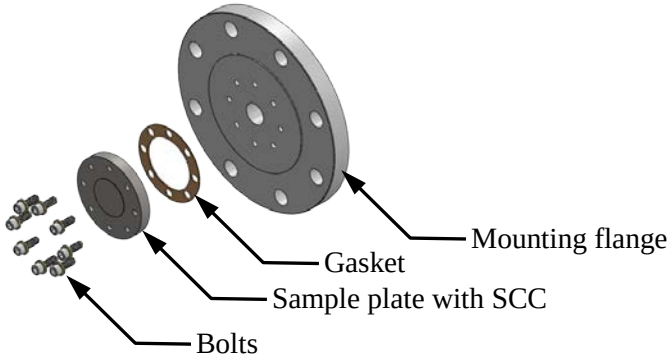

Figure 11. Assembly of an SCC sample.

2.2.3.1 Weld Analysis

A high-fidelity finite element model of the sample plate weld process is under construction to predict the residual stress in the stress corrosion test specimen. The problem is solved using Sandia National Laboratories' Sierra Mechanics code suite, which is composed of several specialized applications

operating either in standalone mode or coupled with each other. Here, the coupled thermomechanical calculation is performed using the thermal conduction application ARIA and the mechanical application ADAGIO. The two applications are loosely coupled using the ARPEGGIO utility [Subia *et al.*, 2017]. The thermal portion of the calculation moves a monolithic hotspot over the volume of the part. The thermal history generated by the model is coupled to visco-plastic constitutive models that include dynamic strain aging to predict residual stress and deformation after a weld. The model will be compared to existing temperature and residual stress measurements on a similar process to confirm that the predicted values are realistic. Adjustments to the weld path can then be simulated to better match the desired prototypic stress field.

A preliminary finite element mesh of the flange and a thermal model have been constructed. The finite element mesh shown in Figure 12 contains a fine hex mesh near the weld to resolve the thermal gradients. The rest of the mesh is course to maximize the efficiency of the model.

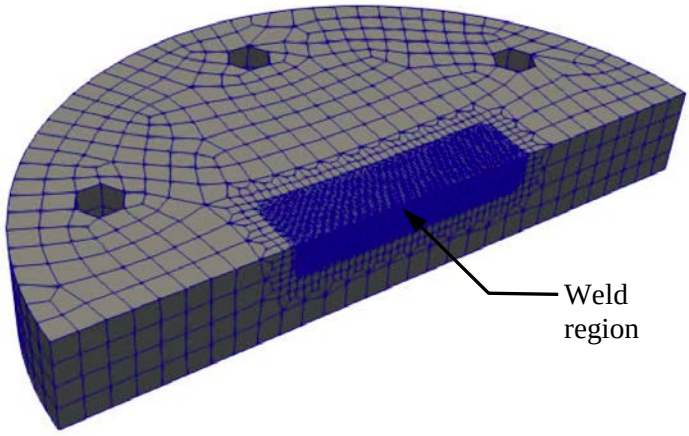

Figure 12. Finite element mesh of the sample plate weld.

2.3 Instrumentation

The following instrumentation will be used to characterize these tests. All stated uncertainties are assumed to represent 95% confidence intervals unless otherwise stated.

2.3.1 Pressure

Pressure will be monitored on the upstream side using a 1034 kPa (150.0 psia) Setra Model ASM transducer and on the downstream side with a 103 kPa (15.0 psia) Model ASM transducer. The pressure in the tank will be monitored with a 2068 kPa (300 psia) Setra Model ASM transducer. The accuracy of the Setra Model ASM transducers is <±0.05% full scale (FS). A summary of all pressure transducers is given in Table 1.

Table 1. Summary of pressure transducers.

Location	Model No.	Range (kPa)	Uncertainty (kPa)
Storage tank	ASM1-300P-A-1M-2C-03-A-01	0 – 2068	1.03
Upstream	ASM1-150P-A-1M-2C-03-A-01	0 – 1034	0.52
Downstream	ASM1-015P-A-1M-2C-03-A-01	0 – 103	0.05

2.3.2 Temperature

All temperature measurements will be taken with K-Type thermocouples. The suggested, combined uncertainty in these measurements including data acquisition, cabling, and positioning errors is 1% of the reading in Kelvin.

2.3.3 Gas Mass Flow Rate

The blowdown flow rate from the tank into the test section will be measured by a mass flow meter (OMEGA Model FMA-1609A, 0 to 50 slpm). The standard liter per minute (slpm) is defined as one liter of air flow at standard conditions of 101.325 kPa and 25 °C (*i.e.* reference density of 1.184 kg/m^3).

For the FMA-1600, the reported accuracy is ± (0.8% of reading + 0.2% FS) for a maximum of ± 1% FS.

Table 2. Summary of mass flow instrumentation.

Description	Model No.	Range (slpm)	Range (kg/s)	Uncertainty (kg/s)
Storage tank to upstream	FMA-1609A	0 – 50	$0 – 9.9\times10^{-4}$	$0 – 1\times10^{-5}$

2.3.4 Aerosol Spectrometer

The Palas Promo® 3000 HP is a flexible, light-scattering aerosol spectrometer system that uses twin sensors to determine quasi-simultaneous particle concentration and particle size at two locations. Fiber-optic cables (light wave conductor or LWC) are used to carry light from the main controller to the remote welas® 2070 high pressure aerosol sensors as well as the resulting light-scattering signal from the remote sensors back to the main controller. The technical parameters of this system are summarized in Table 3. The high-pressure aerosol sensor directly samples gas streams at native pressures up to 1,000 kPa. Rapid fiber optic switching allows a single instrument to analyze the upstream and downstream aerosol sensors in quasi-simultaneous fashion. This sensor range makes reliable measurements possible over the concentration range from < 1 particle/cm^3 to 10^6 particles/cm^3. The instrument is ideally suited to simultaneously monitor the aerosols from the high-pressure upstream and low-pressure downstream side of the simulated crack for aerosol size and concentration characterization.

Table 3. Summary of Palas Promo 3000 HP and welas 2070 HP technical parameters.

Aerosol measurement range	0.2 – 100 μm (selectable)
Minimum Particle Concentration	1.0 particle/cm^3
Maximum Particle Concentration	10^6 particles/cm^3
Maximum Sample Pressure	1,000 kPa
Maximum Sample Temperature	120 °C

2.4 Selection of Initial Conditions

2.4.1 Surrogate Selection

Cerium oxide (CeO_2) will be used as the surrogate for spent nuclear fuel ($\rho_{SNF} \approx 10$ g/cm^3) because of its relatively high density ($\rho_{CeO_2} = 7.22$ g/cm^3) and its commercial availability. Figure 13 shows the particle characteristic size distribution of the surrogate selected for these tests. Here, the distribution is plotted as a function of aerodynamic equivalent diameter (AED). This surrogate was selected because the particles were concentrated in the respirable range (AED < 10 μm). Table 4 gives a summary of the aerosol characteristics of the surrogate.

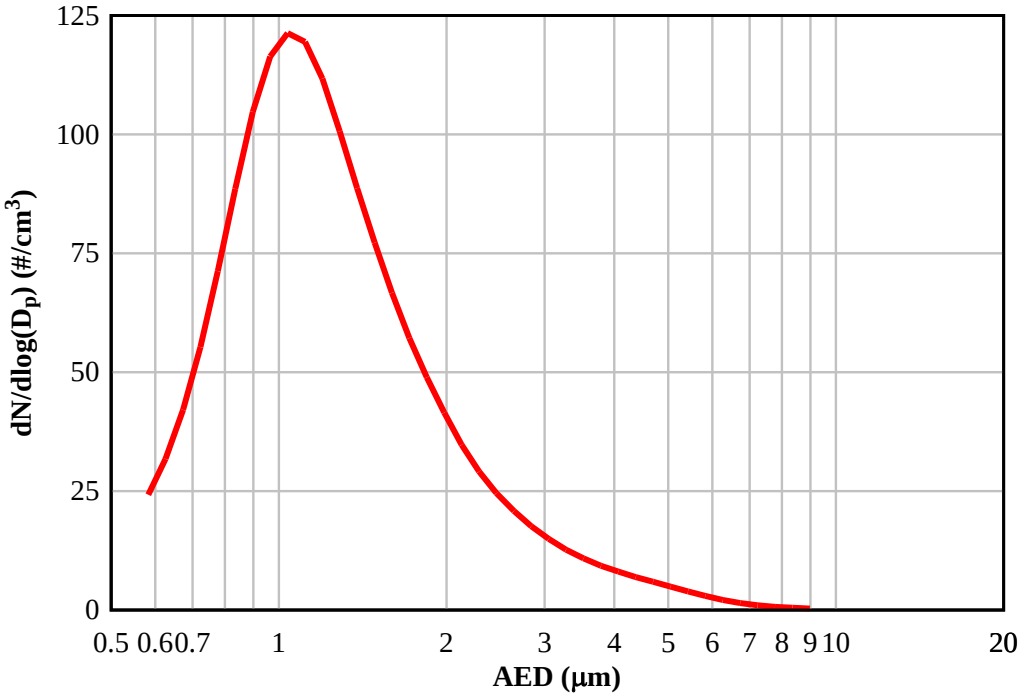

Figure 13. Particle size distribution of the cerium oxide surrogate.

Table 4. Summary of cerium oxide surrogate characteristics.

	Number Particle Size	Mass Particle Size
Median (μm)	1.18	4.12
Mean (μm)	1.36	4.81
Geometric Mean (μm)	1.24	3.98
Mode (μm)	1.07	4.22
Geometric Std. Dev.	1.47	1.88
Total Concentration	2422 (#/cm^3)	2.30 (mg/m^3)

2.4.2 Selection of Aerosol Density

An estimate of the aerosol density is needed to inform the execution of the tests. As described earlier, the proposed tests are focused on respirable particles with an AED < 10 μm. To derive an aerosol density of interest, data from a previous study was referenced to estimate an upper bound for release of spent fuel into a canister [Hanson *et al.*, 2008]. An average release fraction across all tests was found to be 1.9×10^{-5}, where air was blown through segments of spent fuel rods and the released fuel was measured. Of this release fraction, the respirable fraction from all available data was 6.0×10^{-3}. Therefore, the respirable release fraction was estimated as the product of the two fractions to be 1.1×10^{-7}.

To estimate an upper aerosol density for spent fuel dry storage, a canister with 37 pressurized water reactor (PWR) assemblies with a mass of fuel (UO_2) 520 kg per assembly was assumed. Ten percent of the fuel was assumed to fail due to an undefined event. The fines released were assumed to recirculate within the canister without any deposition. The canister was assumed to have a starting initial pressure of 800 kPa (116 psia). The equivalent aerosol density for this assumed system at standard temperature and pressure is approximately 7 mg/m^3. For the storage tank, approximately 50 mg will be needed to achieve an equivalent aerosol density. Previous testing was started with an excess (~ 100 mg) of the respirable ceria particles aerosolized into the tank because of large losses during seeding operations [Durbin *et al.*, 2018]. Improvements for loading the particles with a modified seed generator and keeping them lofted in the pressure tank with internal mixing fans are planned for subsequent testing.

3 SUMMARY

Initial testing using engineered microchannels with characteristic dimensions like those in SCCs revealed several limitations in the available aerosol instrumentation [Durbin *et al.*, 2018]. This report outlines near-term improvements to the apparatus for the measurement of flow rates and aerosol retention in SCCs. Additional considerations are being explored to develop mountable sample plates with laboratory-grown SCCs. The proposed research is summarized below.

Near-term studies:

- Incorporate new aerosol analysis system (Palas Promo® 3000 HP with two welas® 2070 HP sensors)
    - Monitor upstream and downstream samples quasi-simultaneously
    - Record aerosol size distributions at high and low pressures natively
    - Eliminate instrument and sample line biases
- Improve particle loading process
    - Actively mix aerosols inside pressure tank
    - Inject aerosol particles with a modified seed generator
- Simple slot orifice
    - Repeat testing using new aerosol system
- Offset slot orifice
    - Test effect of tortuosity in simplified, controlled manner

Future studies:

- Grow mountable SCCs under accelerated, laboratory conditions
    - Develop weld model
        - Predict residual stress
    - Develop procedures for accelerated SCC growth in sample plates
- Mount and test SCCs in aerosol transmission apparatus

This page is intentionally left blank.

4 REFERENCES

Breimesser, M., S. Ritter, H.P. Seifert, T. Suter, and S. Virtanen, "Application of Electrochemical Noise to Monitor Stress Corrosion Cracking of Stainless Steel in Tetrathionate Solution Under Constant Load," **Corrosion Sci.**, ***63***, 129-139, (2012).

Durbin, S.D., E.R. Lindgren and R.J.M. Pulido, "Measurement of Particulate Retention in Microchannel Flows", SAND2018-10522R, Sandia National Laboratories, Albuquerque, NM, September 19, 2018.

EPRI, "Flaw Growth and Flaw Tolerance Assessment for Dry Cask Storage Canisters," EPRI 3002002785 Electric Power Research Institute, Palo Alto, CA, October (2014).

EPRI., "Dry Cask Storage Welded Stainless Steel Canister Breach Consequence Analysis Scoping Study," EPRI 3002008192, Electric Power Research Institute, Palo Alto, CA, November (2017).

Hanson, B.D., R.C. Daniel, A.M. Casella, R.S. Wittman, W. Wu (BSC), P.J. MacFarlan, and R.W. Shimskey, "Fuel-In-Air FY07 Summary Report," PNNL-17275, Pacific Northwest National Laboratory, Richland, Washington, September (2008).

Lewis, S., "Solid Particle Penetration into Enclosures", J. Hazardous Materials, *43*, 195-216, (1995).

Liu, D-L.and W.W. Nazaroff, "Modeling Pollutant Penetration Across Building Envelopes," **Atmos. Environm**., ***35,*** 4451-4462, (2001).

Liu, D-L. and W.W. Nazaroff, "Particle Penetration Through Building Cracks," **Aerosol Science and Technology**, ***37***, 565-573, (2003).

Meyer, R. M., *et al.*, "Evaluating Conventional NDE Methods for Crack Detection in Metal Canisters," Presentation at *Extended Storage Collaboration Program (ESCP)*, December 4, (2013).

Mosely, R.B., D.J. Greenwell, L.E. Sparks, Z. Guo, W.G. Tucker, R. Fortmann, C. Whitfield, "Penetration of Ambient Fine Particles into the Indoor Environment," **Aerosol Science and Technology**, ***34***, 127-136, (2001).

Powers, D.A., "Aerosol Penetration of Leak Pathways – An Examination of the Available Data and Models," SAND2009-1701, Sandia National Laboratories, Albuquerque, NM, April (2009).

Schindelholz, E., C. Bryan, and C. Alexander, "FY17 Status Report: Research on Stress Corrosion Cracking of SNF Interim Storage Canisters," SAND2017-10338R, Sandia National Laboratories, Albuquerque, NM, August (2017).

Subia, S.R., J.R. Overfelt and D.G. Baur, "SIERRA Code Coupling Module: Arpeggio User Manual – Version 4.44," SAND2017-3777, Sandia National Laboratories, Albuquerque, NM, April 13, 2017.